END

FILMED

DTIC

# MICROCOPY RESOLUTION TEST CHART
NATIONAL BUREAU OF STANDARDS-1963-A

# A Comparison of Quantum, Classical, and Semiclassical Descriptions of a Model, Collinear, Inelastic Collision of Two Diatomic Molecules

M. PAGE, E. S. ORAN AND J. P. BORIS

*Laboratory for Computational Physics*

D. MILLER AND R. E. WYATT

*Department of Chemistry*
*University of Texas at Austin*
*Austin, TX 78712*

H. RABITZ

*Department of Chemistry*
*Princeton University*
*Princeton, NJ 05840*

B. A. WAITE

*Department of Chemistry*
*U. S. Naval Academy*
*Annapolis, MD 21402*

December 13, 1985

AD-A162 357

DTIC
ELECTE
DEC 1 3 1985
S          D
B

NAVAL RESEARCH LABORATORY
Washington, D.C.

DTIC FILE COPY

85   12   13   040

A 162 357

# REPORT DOCUMENTATION PAGE

| 1a. REPORT SECURITY CLASSIFICATION <br> UNCLASSIFIED | | 1b. RESTRICTIVE MARKINGS | | | |
|---|---|---|---|---|---|
| 2a. SECURITY CLASSIFICATION AUTHORITY | | 3. DISTRIBUTION / AVAILABILITY OF REPORT <br><br> Approved for public release; distribution unlimited. | | | |
| 2b. DECLASSIFICATION / DOWNGRADING SCHEDULE | | | | | |
| 4. PERFORMING ORGANIZATION REPORT NUMBER(S) <br><br> NRL Memorandum Report 5700 | | 5. MONITORING ORGANIZATION REPORT NUMBER(S) | | | |
| 6a. NAME OF PERFORMING ORGANIZATION <br><br> Naval Research Laboratory | 6b. OFFICE SYMBOL <br> (If applicable) <br> Code 4040 | 7a. NAME OF MONITORING ORGANIZATION <br><br> Office of Naval Research | | | |
| 6c. ADDRESS (City, State, and ZIP Code) <br><br> Washington, DC 20375-5000 | | 7b. ADDRESS (City, State, and ZIP Code) <br><br> Arlington, VA 22217 | | | |
| 8a. NAME OF FUNDING / SPONSORING ORGANIZATION <br><br> Office of Naval Research | 8b. OFFICE SYMBOL <br> (If applicable) | 9. PROCUREMENT INSTRUMENT IDENTIFICATION NUMBER | | | |
| 8c. ADDRESS (City, State, and ZIP Code) <br><br> Arlington, VA 22217 | | 10 SOURCE OF FUNDING NUMBERS | | | |
| | | PROGRAM ELEMENT NO <br> 61153N | PROJECT NO | TASK NO. <br> RR0B064F | WORK UNIT ACCESSION NO <br> DN155-537 |

11. TITLE (Include Security Classification)  A Comparison of Quantum, Classical, and Semiclassical Descriptions of a Model, Collinear, Inelastic Collision of two Diatomic Molecules

12. PERSONAL AUTHOR(S)
Page, M., Oran, E.S., Boris, J.P., Miller, D.,* Wyatt, R.E.,* Rabitz, H.,† and Waite, B.A.§

| 13a. TYPE OF REPORT <br> Interim | 13b. TIME COVERED <br> FROM _____ TO _____ | 14 DATE OF REPORT (Year, Month, Day) <br> 1985 December 13 | 15 PAGE COUNT <br> 49 |
|---|---|---|---|

16. SUPPLEMENTARY NOTATION    *Department of Chemistry, University of Texas at Austin, Austin, TX 78712
†Department of Chemistry, Princeton University, Princeton, NJ 05840
(Continues)

| 17 | COSATI CODES | | 18. SUBJECT TERMS (Continue on reverse if necessary and identify by block number) |
|---|---|---|---|
| FIELD | GROUP | SUB-GROUP | Molecular scattering,    Collision dynamics <br> Vibrational energy transfer    Collinear collision |
| | | | |

19. ABSTRACT (Continue on reverse if necessary and identify by block number)

The collinear dynamics of a model diatom-diatom system is investigated. The collision partners are harmonic oscillators for which the masses and force constants are chosen to correspond to those of the nitrogen and oxygen molecules. The interaction between the molecules arises from a Lennard-Jones 6-12 potential acting between the inside atoms in the collinear system.

Quantum mechanical close coupled calculations are performed for several collision energies ranging from 1.0 ev to 2.25 ev. The state-to-state transition probabilities which are extracted from these calculations are then used as a benchmark for comparison. Semiclassical calculations are performed within the framework of a classical path approximation. A simple scheme to modify the classical path to reflect energy exchange between the collision coordinate and the internal degrees of freedom is found to improve the results. On the whole, the agreement between the semiclassical and the quantum mechanical results is surprisingly good. The classical trajectory calculations correctly display many of the qualitative features of the collisions but the numerical agreement is not as close. Unexpectedly, the classical results do not appear to be improving as the collision energy is increased.

| 20. DISTRIBUTION / AVAILABILITY OF ABSTRACT <br> ☒ UNCLASSIFIED/UNLIMITED  ☐ SAME AS RPT  ☐ DTIC USERS | 21. ABSTRACT SECURITY CLASSIFICATION <br> UNCLASSIFIED | |
|---|---|---|
| 22a. NAME OF RESPONSIBLE INDIVIDUAL <br> Michael J. Page | 22b. TELEPHONE (Include Area Code) <br> (202) 767-2118 | 22c. OFFICE SYMBOL <br> Code 4040 |

**DD FORM 1473,** 84 MAR         83 APR edition may be used until exhausted.
All other editions are obsolete.

i
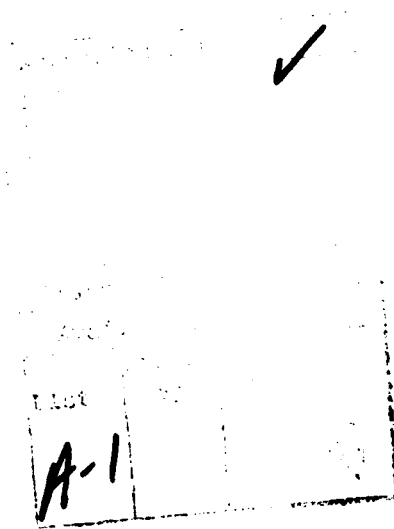
16. SUPPLEMENTARY NOTATION (Continued)

§ Department of Chemistry, U.S. Naval Academy, Annapolis, MD 21402

CONTENTS

iii

# A COMPARISON OF QUANTUM, CLASSICAL, AND SEMICLASSICAL DESCRIPTIONS OF A MODEL, COLLINEAR, INELASTIC COLLISION OF TWO DIATOMIC MOLECULES

## I. Introduction

Molecular dynamics simulations involving a relatively large number of molecules are becoming an increasingly powerful tool for the study of both gas and condensed phase phenomena. There has been considerable progress in the ability to simulate a variety of equilibrium and nonequilibrium situations and in calculating, for example, transport properties (1). This progress is due both to the improved computational facilities and improved methods of doing the calculations.

There is a now interest in using molecular dynamics to describe the interaction of a shock wave and a condensed phase material. The motivation for this approach is based on the observation that the region immediately behind the shock wave is not in equilibrium. Thus molecular dynamics might be used when the usual fluid descriptions, which assume equilibrium equations of state, transport processes, and reaction rates, are not valid. Typical molecular dynamics simulations (3) describe the time evolution of the dynamical state of the system by solving the classical equations of motion. These calculations incorporate all of the interparticle interactions as accurately as possible. For most applications, this classical approximation to the dynamics is justified because typical quantum mechanical interference effects (e.g.,resonant cross sections) tend to be averaged out in systems possessing many degrees of freedom (4).

---

Under some circumstances however, there might be residual quantum mechanical effects, even though a statistical average is taken. This paper presents the preliminary work done to develop phenomenological models of vibrational energy exchange which can be incorporated into large scale classical simulations. These models might be designed, for example, to incorporate some of the effects of discrete vibrational excitations, and thus test when they might be important in the calculation. The first step in developing such models is a careful comparison between representative classical and quantum calculations, such as presented here.

## II. Background to Present Research

Due to practical computational limitations, most molelcular dynamics studies treat molecules as rigid bodies (5). While this approach precludes the possibility of vibrational energy exchange, it does incorporate the very important dynamical effects of rotational and translational energy exchange though molecular collisions. There are many examples in the literture of simulations involving various shapes of rigid molecules (6). The inter-action between molecules is generally taken as a sum of pairwise additive, point interactions usually (but not always (7)) acting between atomic centers. The equations of motion are most efficiently integrated in a cartesian coordinate system with a series of holonomic constraints imposed to reproduce the molecular structure (5).

Some dynamics simulations have included vibrational degrees of freedom explicitly (see for example, reference (9)). This requires a knowledge of not only the intermolecular interactions (including their angular dependences), but also a knowledge of the intramolecular potential as a function of the nuclear coordinates. Explicitly including the vibrational

2

degrees of freedom might also allow for the additional reactive processes of bond dissociation or association (10). A disadvantage of this approach is the requirement of treating all degrees of freedom on the same dynamical footing, i.e., classically. While the classical treatment of the translational and rotational motions is generally an excellent approximation, the vibrational interactions begin to become less reliable (8).

A further disadvantage of explicitly including all degrees of freedom in a molecular dynamics simulation is the problem of temporally resolving the rapid internal vibrations. This requires an integration time step on the order of 1/40 of a vibrational period for systems with strong but realistic bond potentials (9). Some studies have avoided this problem by including artificially soft bonds, which vibrate at a low frequency (10,11). The less rigorous rigid-body type of simulation can accomodate a larger time step in the numerical solution of the classical equations of motion, consequently a longer period of time can be simulated. In addition, there are generally fewer equations of motion since there are fewer degrees of freedom.

The goal of the present research program is to investigate ways in which the effects of the vibrational degrees of freedom might be included within the framework of the computationally tractable rigid body approach to molecular dynamics simulations. Of particular interest eventually is the determination of the influence of the vibrational degrees of freedom on the accumulation of internal energy and subsequent bond dissociation. The initial step in such a study must be a determination of the quality of a classical or semiclassical treatment of a vibrationally inelastic molecular collision. Such a determination can be made by comparing an exact quantum calculation to the corresponding classical and semiclassical treatments.

3

Previous work in comparing quantum, semiclassical and classical methods for treating molecular collision phenomena has been motivated primarily by interest in ascertaining the correspondence between classical mechanics and quantum mechanics (12). The motivation for the present work stems from the need to incorporate, within the classical framework of dynamics simulations, the important effects arising from vibrational energy exchange, quantum effects due to interference, and the effects arising from dissociation.

Apart from the computational advantage of the classical approach to molecular dynamics, it also possesses the advantage of allowing one to follow the "trajectories," especially through the important interaction region. Quantum dynamical treatments allow one to "look" at the physically measurable quantities only before and after collision, preventing intuitive insight into the effect of a third body or other perturbations which might interrupt the two body interaction. Such information from quantum calculations would be extremely useful, and attempts have been made previously to address this question (13).

The first step in the present work is the selection of the particular model molecular collision problem to serve as a benchmark for investigation. The model chosen involves the collinear inelastic collision between diatomic molecules, the details of which are described in section III. Transition probabilities are determined quantum mechanically, semiclassically (using a classical path approximation) and classically. The precise methodologies used are described in section IV. The results are presented and compared in section V. The last section contains a discussion of the results and how they impact on the question of improvement of molecular dynamics simulations.

4

III. The Model Problem

The problem we consider is a collinear collision between two homo-
nuclear diatomic molecules. Each molecule is represented as a harmonic
oscillator. The masses and force constants are chosen to correspond to
those of the oxygen and nitrogen molecules. The intermolecular interaction
arises from a Lennard-Jones potential acting between the inside atoms in the
collinear system. Thus only adjacent atoms interact. This is illustrated
schematically in Fig. I, where the atoms are labeled a,b,c and d and the
potential between atoms can be written:

$$V_{ab}(r_1) = \frac{k_1}{2} (r_1 - r_{10})^2 \qquad (1a)$$

$$V_{cd}(r_2) = \frac{k_2}{2} (r_2 - r_{20})^2 \qquad (1b)$$

$$V_{bc} = 4\varepsilon \left\{ \left( \frac{\sigma}{R_{bc}} \right)^{12} - \left( \frac{\sigma}{R_{bc}} \right)^6 \right\} \qquad (1c)$$

$$V_{ac} = V_{ad} = V_{bd} = 0 \qquad (1d)$$

where $r_{10}$ and $r_{20}$ are the equilibrium separations of the molecules ab and bc
respectively. The separation between the centers of mass of the two
molecules is denoted by R,

$$R = R_{bc} + 1/2(r_1 + r_2)$$

The harmonic force constants are denoted $k_1$ and $k_2$. $\sigma$ and $\varepsilon$ are the Lennard
Jones distance and energy parameters respectively. For the problem
considered here,

5

$$r_{10} = 2.282 \text{ bohr} \qquad k_1 = 20.57 \text{ ev}/(\text{bohr})^2$$

$$r_{20} = 2.074 \text{ bohr} \qquad k_2 = 40.09 \text{ ev}/(\text{bohr})^2$$

$$m_a = m_b = 16 \text{ amu} \qquad \sigma = 4.730 \text{ bohr}$$

$$m_c = m_d = 14 \text{ amu} \qquad \varepsilon = .010 \text{ ev}$$

We express the Lennard-Jones potential, which is a function of $R_{bc}$, in terms of the bc separation when the two oscillators are at there equilibrium positions (F), and the small deviations from this value ($x_1$ and $x_2$).

$$F = R - 1/2 \ (r_{10} + r_{20}) \tag{2a}$$

$$x_1 = r_1 - r_{10} \tag{2b}$$
$$x_2 = r_2 - r_{20}$$

Using Eqns. (2) in Eqn. (1c) the Lennard-Jones potential becomes,

$$V_{bc}(F,x_1,x_2) = 4\varepsilon \ \{(\frac{\sigma}{F - \frac{1}{2}(x_1 + x_2)})^{12} - (\frac{\sigma}{F - \frac{1}{2}(x_1 + x_2)})^{6}\}$$

$$\tag{3}$$

$$= 4\varepsilon \ \{(\frac{\sigma}{F})^{12} (1 - \alpha)^{-12} - (\frac{\sigma}{F})^{6} (1 - \alpha)^{-6}\}$$

where,

$$\alpha \equiv 1/2(x_1 + x_2)/F. \tag{4}$$

The kinetic energy, in the center of mass coordinate system, can be written as,

$$T = \frac{p_1^2}{2\mu_{ab}} + \frac{p_2^2}{2\mu_{cd}} + \frac{p^2}{2\mu_{ab,cd}}. \tag{5}$$

6

where $p_1$, $p_2$, and P are the momenta conjugate to $r_1$, $r_2$, and R and the reduced masses are defined as,

$$\mu_{ab} = \frac{m_a m_b}{m_a + m_b} \qquad\qquad \mu_{cd} = \frac{m_c m_d}{m_c + m_d}$$

(6)

$$\mu_{ab,cd} = \frac{(m_a + m_b)(m_c + m_d)}{m_a + m_b + m_c + m_d}$$

The Hamiltonian for the model system is thus,

$$H = (\frac{p_1^2}{2\mu_{ab}} + \frac{1}{2} k_1 x_1^2) + (\frac{p_2^2}{2\mu_{cd}} + \frac{1}{2} k_2 x_2^2) + \frac{P^2}{2\mu_{ab,cd}} + V_{LJ}(R_{bc})$$

(7)

$$= H^{\circ} + \frac{P^2}{2\mu_{ab,cd}} + V_{LJ}(R_{bc})$$

IV.  Theoretical Approaches to the Scattering Problem

A.  Quantum Mechanical Description

Since the Hamiltonian for the system does not depend on time, we search for stationary state solutions of the Schroedinger equation.  In the quantum mechanical treatment of inelastic scattering, it is convenient to work with a complete set of functions of the internal coordinates $r_1$ and $r_2$.  The scattering wavefunction, which is a function of the three coordinates $r_1$, $r_2$ and R, is then written as a linear expansion in this set of functions, where the expansion coefficients are functions of R.

$$\Psi_p(R,r_1,r_2) = \sum_n f_{pn}(R)\phi_n(r_1,r_2)$$

(8)

7

The set of functions $\{\phi_n(r_1,r_2)\}$ is chosen to be the eigenfunctions of the internal portion of the Hamiltonian. Since the internal portion of the Hamiltonian is the sum of two harmonic oscillator Hamiltonians, the eigenfunctions are simply products of harmonic oscillator eigenfunctions.

$$H^{o}(r_1,r_2)\ \phi_n(r_1,r_2)\ E_n \phi_n(r_1,r_2) \tag{9}$$

where

$$\phi_n(r_1,r_2) = \phi_i(r_1)\phi_j(r_2) \tag{10}$$

and

$$E_n = E_i + E_j = (i + \tfrac{1}{2})\hbar(\frac{k_1}{\mu_{ab}})^{1/2} + (j + \tfrac{1}{2})\hbar(\frac{k_2}{\mu_{cd}})^{1/2} \tag{11}$$

The index $n$ specifies the state of both molecules, i.e. specifies $i$ and $j$. The time independent Schroedinger equation for the entire system is,

$$[\frac{-\hbar^2}{2\mu_{ab,cd}}\ \frac{d^2}{dR^2} + V_{bc}(R,r_1,r_2) + H^{o}(r_1,r_2)]\ \sum_n f_{np}(R)\ \phi_n(r_1,r_2)$$

$$= E \sum_n f_{pn}(R)\ \phi_n(r_1,r_2) \tag{12}$$

Multiplying on the left by $\phi_\ell(r_1,r_2)$ and integrating over the internal coordinates, $r_1$ and $r_2$ yields the following set of coupled equations for the expansion coefficients $f_{p\ell}(R)$,

$$\frac{d^2}{dR^2}\ f_{p\ell}(R) = \frac{2\mu_{ab,cd}}{\hbar^2}\ (E_\ell - E)f_{p\ell}(R) + \sum_n V_{\ell n}(R)f_{pn}(R) \tag{13}$$

8

where

$$V_{\ell n}(R) = \int\int \phi_\ell^*(r_1,r_2) V_{bc}(R,r_1,r_2)\, \phi_n(r_1,r_2) dr_1 dr_2 \qquad (14)$$

Eqn. (13) can be rewritten in matrix form as,

$$\frac{d^2}{dR^2}\, \underline{f}(R) = \underline{D}(R)\underline{f}(R) \qquad (15)$$

with the symmetric matrix D defined by,

$$D_{ij} = D_{ji} = \frac{2u_{ab,cd}}{\hbar^2}\, [V_{ij}(R) + (E_i - E)\delta_{ij}] \qquad (16)$$

The coupled equations (Eq. 13) are solved numerically by the R-matrix method (14). The essential idea of the method is to solve the problem in the interaction region where the basis states are coupled to one another and then to match this wavefunction with the known uncoupled asymptotic forms. The solution in the interaction region is determined by dividing the R-space into many sectors within which the coupling potential does not change significantly. Within each sector, the unitary transformation is found which diagonalizes the coupling matrix D.

$$\underline{U}^+(R)\, \underline{D}(R)\underline{U}(R) = \underline{D}'(R) \qquad (17)$$

Equation (15) may then be written within each sector in the uncoupled form,

$$\frac{d^2}{dR^2}\, \underline{f}'(R) = \underline{D}'\underline{f}(R) \qquad (18)$$

where

9

$$\underline{f}'(R) = \underline{U}^{+}(R)\underline{f}(R) \qquad\qquad (19)$$

and $D'$ is a diagonal matrix. The solution is then matched at adjacent

sectors, ensuring the continuity of the wavefunction and its derivative.

Formally, the summations over n in Eqns. (12) and (13) extend to

infinity. This is because an infinite number of the functions $\phi_n(r_1,r_2)$ are

required to form a complete set of functions which span the space of $r_1$ and

$r_2$. The choice of internal state eigenfunctions to represent this space is

a judicious one however, since it is expected that even in the interaction

region, the oscillators will to some extent retain their identity. In

practice we do a finite basis set expansion. Functions are selected on the

basis of their energy, and the calculations are performed until increasing

the length of the expansion has no effect on the answer.

To solve the Schroedinger Equation, we need to know the elements of the

coupling matrix defined in Eqn. (14) as a function of the molecular separa-

tion R. This requires either the calculation of N-squared integrals (N is

the number of basis states) each time a different value of R is considered

during the course of the calculation, or the prior storage of a large amount

of R-dependent data. To avoid the storage problem and to simplify the inte-

gral computation, we use the following scheme for evaluating the matrix

elements of the Lennard-Jones potential.

In Eqn. (3), the Lennard-Jones potential acting between the inside atoms

was written so as to separate the dependence of the potential on the inter-

nal coordinates (the $\alpha$ dependence) from the dependence on the collision

coordinate (the $\Gamma$ dependence). For a given molecular separation, we can now

expand the potential about the equilibrium positions of the oscillators.

Thus equation (3) is expanded in a Taylor series in $\alpha$ about the point $\alpha=0$.

10

$$V(F,x) = V(F,x=0) + \left(\frac{dV}{d\alpha}\right)_{\alpha=0} \alpha + \frac{1}{2!}\left(\frac{d^2V}{d\alpha^2}\right)_{x=0} x^2 + \ldots \quad (20)$$

Carrying the expansion to fourth order and integrating over the internal coordinates, the coupling matrix V becomes,

$$
\begin{aligned}
V(F) = 4\varepsilon[(\tfrac{\sigma}{F})^{12} - (\tfrac{\sigma}{F})^6] \, \underset{\sim}{1} \quad &+ \quad 4\varepsilon[12(\tfrac{\sigma}{F})^{12} - 6(\tfrac{\sigma}{F})^6] \, \underset{\sim}{A}^{(1)}/2F \\
&+ \quad 4\varepsilon[78(\tfrac{\sigma}{F})^{12} - 21(\tfrac{\sigma}{F})^6] \, \underset{\sim}{A}^{(2)}/2F \\
&+ \quad 4\varepsilon[364(\tfrac{\sigma}{F})^{12} - 56(\tfrac{\sigma}{F})^6] \, \underset{\sim}{A}^{(3)}/2F \\
&+ \quad 4\varepsilon[1365(\tfrac{\sigma}{F})^{12} - 126(\tfrac{\sigma}{F})^6] \, \underset{\sim}{A}^{(4)}/2F
\end{aligned}
$$

$$(21)$$

with the matrices $A^{(n)}$ defined as,

$$\underset{\sim}{A}^{(n)}_{ij} = \iint \Phi_i(r_1,r_2)(x_1+x_2)^n \Phi_j(r_1,r_2)dr_1,dr_2 \quad (22)$$

The important point is that these matrices, and hence the integrals which make up the coupling elements, have no dependence on the collision coordinate. The coupling matrix is obtained as a function of R by multiplying these previously stored matrices by the R-dependent coefficients shown in Eqn. (21). We have found that the coupling matrix is well converged when the expansion of the Lennard-Jones potential is carried out to fourth order. As an additional test, we have performed a number of classical trajectory calculations using this truncated expansion of the potential. Again, the fourth order expansion produces results which are the same as the analytical form for the potential to four decimal places.

11

### 3. Semiclassical Description

The semiclassical method we have chosen is generally referred to as a classical path approach. The underlying idea is that motion along a collision coordinate is responsible for initiating transitions among the discrete quantum states of the colliding partners, but that this motion is essentially classical in nature. One first chooses a reasonable mean trajectory for the collisional degree of freedom. This trajectory could be, for example, a classical trajectory associated with a hypothetical system for which the internal degrees of freedom have been frozen. Since the interaction among the collision partners is a function of the collision coordinate, this predetermined trajectory provides the interaction potential as a function of time. Using this interaction potential, one then constructs a time dependent Hamiltonian operator for the internal degrees of freedom. The time dependent Schroedinger equation is then solved in the subspace of the internal degrees of freedom.

For our model problem, we first separate the Hamiltonian into a portion which contains all of the internal coordinate dependence and a portion which depends upon the collision coordinate only,

$$H = \{\frac{-\hbar^2}{2\mu_{ab,cd}} \frac{d^2}{dR^2} + V(R,r_0)\} + \{H^0 + V(R,r) - V(R,r_0)\} \quad (23)$$

The first set of brackets contain a simple Hamiltonian for the collision coordinate. We solve this one dimensional problem classically to obtain the collision coordinate R as a function of time. The second set of brackets contain a Hamiltonian for the internal degrees of freedom. The collision coordinate appears as a parameter in this Hamiltonian, its time dependence having been pre-determined. The equation which must be solved is then

12

$$i\hbar \frac{\partial \Psi(r_1,r_2,t)}{dt} = [H^O + V(R,r) - V(R,r_o)] \, \Psi(r_1,r_2,t) \quad (24)$$

As in the close coupling calculations, we expand the wavefunction in a basis of eigenstates of $H^O$, the harmonic oscillator product functions.

$$\Psi(r_1,r_2,t) = \sum_j \Phi_j(r_1,r_2) \chi_j(t)$$

$$\quad (25)$$

$$= \sum_j \Phi_j(r_1,r_2) \, (\alpha_j(t) + i\beta_j(t))$$

Left multiplying Eqn. (24) by one particular eigenfunction and integrating over the internal coordinates produces equations describing the time dependence of the real and imaginary components of the expansion coefficients:

$$\hbar \frac{\partial \alpha_j}{dt} = \{E_j - V(R,r_o)\}\beta_j + \sum_k V_{jk}\beta_k$$

$$\quad (26)$$

$$\hbar \frac{\partial \beta_j}{dt} = \{E_j - V(R,r_o)\}\alpha_j - \sum_k V_{jk}\alpha_k$$

These equations can then be solved numerically. A typical calculation begins with the a large separation between the two molecules with unit probability of being in one of the internal eigenstates (entrance channels). The system then proceeds through the interaction region and back out to large separation. The square moduli of the expansion coefficients then give the probability that a measurement will find the system in each of the possible exit channels. The validity of the classical path approach is

13

discussed by Child [15]. Essentially what is found is what one intuitively
expects. The change in momentum associated with transitions among various
diabatic states should be small relative to the momentum associated with the
collision coordinate. In other words, the classical paths associated with
different entrance and exit channels should all lie close to the assumed
path.

## C. Classical Description

The classical description of the inelastic scattering is also based on
the Hamiltonian of Eqn. (7). While classical trajectories governed by this
Hamiltonian are straightforward to calculate (16), it is less clear how to
compare the trajectory results with the corresponding quantum mechanical
results. The most widely applied approach for making comparisons between
classical and quantum results is the quasi-classical method (17). Before
applying this approach, a canonical transformation (26) is applied to the
Hamiltonian of Eqn. (7) such that the new internal coordinates and momenta
correspond to the action-angle variables. The action variables are
proportional to the total energy of the oscillators and are therefore
susceptible to being "quantized" in units of Planck's constant (18). The
angle variables then correspond to the phase of the oscillators. For the
harmonic oscillators under consideration, the old internal coordinates and
momenta $(r,p)$ are given in terms of the new action-angle variables $(n,q)$ as:

$$r - r_o = [\frac{2(n+ 1/2)\hbar}{\mu\omega}]^{1/2} \sin q$$

$$(27)$$

$$p = [2(n + 1/2)\hbar\mu\omega]^{1/2} \cos q$$

14

The Hamiltonian of Eqn. (7), in terms of these new conjugate variables, is given by,

$$H(P,R,n_1,n_2,q_1,q_2) = \frac{P^2}{2\mu_{ab,cd}} + V_{LJ}(R,r_1(n_1,q_1),r_2(n_2,q_2))$$

$$(28)$$

$$+ (n_1 + 1/2)\,\hbar\omega_1 + (n_2 + 1/2)\,\hbar\omega_2$$

A useful property of the internal action-angle variables is that in the asymptotic region, where the interaction potential vanishes, the Hamiltonian (Eqn. (28)) becomes independent of the new angle variables. Hamilton's equations of motion, given by,

$$\frac{\partial H}{\partial n_1} = \dot{q}_1 \qquad -\frac{\partial H}{\partial q_1} = \dot{n}_1$$

$$\frac{\partial H}{\partial n_2} = \dot{q}_2 \qquad -\frac{\partial H}{\partial q_2} = \dot{n}_2 \qquad (29)$$

$$\frac{\partial H}{\partial P} = \dot{R} \qquad -\frac{\partial H}{\partial R} = \dot{P}$$

therefore imply that the action variables (i.e., the internal oscillator energies) become constants of the motion both before and after collision.

The major obstacle in making comparisons between classical and quantum mechanical results is the fact that the classical action variables (i.e., the classical counterpart of the vibrational quantum numbers) are allowed to have a continuous range of values, whereas the quantum mechanical oscillators are allowed to have only discrete values for quantum numbers (i.e., integers). The crux of the quasi-classical approach (also known as the

15

"binning" or "histogram" method) is simply to assign final (asymptotic) non-integer values of the action variables to the nearest integer value. In practice, a large number of trajectories are calculated, each trajectory is subsequently "binned", and a statistical analysis is performed on the results of binning the "batch" of trajectories.

Trajectories begin in the asymptotic region, where the variables are assigned the following initial conditions (assuming a total collision energy E):

$$
\begin{aligned}
R &= \text{large} \\
n_1 &= \text{integer (corresponding to initial quantum state)} \\
n_2 &= \text{integer (corresponding to initial quantum state)} \\
P &= [2\mu_{ab,cd}(E - (n_1 + 1/2)\hbar\omega_1 - (n_2 + 1/2)\hbar\omega_2)]^{1/2} \\
q_1 &= \text{random } (0,2\pi) \\
q_2 &= \text{random } (0,2\pi).
\end{aligned}
\tag{30}
$$

The angle variables (i.e., the initial oscillator phases) are chosen randomly from a uniform distribution between 0 and $2\pi$. A large number of trajectories simulates, to a close approximation, all of the possible types of molecular encounters for this collinear model. The equations of motion (Eqn. (29)) are numerically integrated until the collision coordinate becomes large. At this point, the final action variable is assigned to a "bin" corresponding to the quantum final number.

## V. Computational Results

Calculations were performed for total collision energies ranging from 1.0 ev to 2.25 ev. Figure II shows the intermolecular potential acting between atoms b and c. On the same energy scale, the figure also shows the energy level spacings for the two oscillators and the positions of the first several levels of the combined system. Note, for example, that a collision starting in the ground state (0,0) with a total energy of 1.0 ev would have roughly .24 ev as initial internal (vibrational) energy and would thus have about .76 ev as initial translational energy in the collision coordinate. The Lennard-Jones distance parameter, $\sigma = 2.5$ A, is somewhat smaller than the approximately 3.5 A that one might expect to see for a nonbonded inter-action between nitrogen and oxygen. This was done to increase the amount of inelastic scattering at low energies. The indexing scheme for the diatomic product functions is shown in Table I.

As was mentioned earlier, the flexibility in the semiclassical approach is in the choice of the classical path. A strict interpretation of a quantum mechanical description of the scattering event does not recognize the existence of well defined "path" for the collision coordinate along which the system proceeds. We do, however, speak of such a path as it relates to the approximate semiclassical description. As described above, the most obvious choice for this path is a classical trajectory for the collisional degree of freedom with the internal coordinates frozen at their equilibrium values.

Table II displays a comparison, for a particular collision, of quantum mechanical and semiclassical state-to-state probabilities where various classical path approaches were used. The semiclassical calculations at this energy all use 25 basis states. The close coupling calculations use 30. At

17

this energy, 14 of these channels are open. The total energy for the calculation is 1.25 ev. and the oscillators are initially in their ground states. At 1.25 ev, all of the calculations show roughly 90 percent retention probability (elastic scattering).

The first semiclassical column in Table II corresponds to a calculation in which the path is the simple classical trajectory for the collision coordinate. The agreement is at least qualitatively quite good. Note the direction of the deviation. The semiclassical scheme predicts too much inelastic scattering. This deviation can be understood by noting that energy is not conserved in this calculation. The system begins with the minimum allowable energy in the internal vibrations. As the molecules proceed along the classical trajectory, the Hamiltonian for the internal degrees of freedom changes with time reflecting the coupling between the oscillators. This coupling produces an amplitude to find the system in higher energy internal states. Energy is not a constant of the motion for the internal portion of the motion since the Hamiltonian depends on time, but energy is conserved by construction for the collision coordinate. Therefore energy is not conserved for the system as a whole. The molecules can emerge from the collision with appreciable probabilities of being found in higher energy states, yet the molecules translate away from one another with the same kinetic energy that they had during the approach. There is a net adition of energy to the system.

In the collision considered here, a consequence of this energy addition is too much inelastic coupling. As the molecules approach each other and translational energy begins to be transferred to internal vibrational energy, one expects the molecules to slow down. With less energy in the translation, the molecules would not approach as closely and consequently,

18

there would be less coupling. A prediction of the probability for a system starting in a highly excited state to emerge in the ground vibrational state has the opposite problem. Starting with only a small portion of the energy in translation, the trajectory would not provide enough coupling since it cannot reflect a transfer of energy from the internal coordinates to the collision coordinate.

These two probabilities, of a transition from the ground state to a particular excited state and from that excited state to the ground state, are known to be equal by microscopic reversibility. It is then reasonable to symmetrize this probability matrix to impose this feature of the correct physical result. We do this simply by taking the arithmetic mean of two symmetrically disposed probabilities. The diagonal elements, the probabilities of elastic scattering, are then adjusted by the normalization condition. Results, which have been modified in this way are shown in column b of Table II. These are a notable improvement (in comparison to the quantum mechanical calculations) over the probabilities in the first column.

The problem of the lack of energy conservation in semiclassical calculations of this sort is well known. Schemes designed to compensate for this weakness have been proposed, usually by choosing a classical trajectory which is characterized by an energy (19) or velocity (20) averaged between initial and final states. These schemes yield a path which is suitable for the one state-to-state transition of interest. We are interested in simultaneously ascertaining a probability of the system emerging in each of the exit channels given that it began in a particular entrance channel. The above discussion suggests the incorporation of some sort of feedback mechanism in the semiclassical calculations. Perhaps the classical path can be

19

dynamically modified so as to reflect, at least partially, the vibrational-
translational energy transfer. Ideas along these lines have been proposed
in the past, focusing on the coupling of the oscillator response to the
classical path (21) or on the incorporation of an effective potential for
the collision coordinate (22).

The probabilities in the third semiclassical column of table II, column
c, result from a simple incorporation of some "back coupling" of the inter-
nal degrees of freedom to the relative motion of the collision partners.
The classical path at the onset of the collision is the unperturbed classi-
cal trajectory associated with the total collision energy less the internal
energy for the particular entrance channel. The path is modified at each
timestep of the numerical intregration of Eqn. (26) according to an energy
conservation constraint imposed on the system as a whole. Since the time
step can be made arbitrarily small, this corresponds to a continuous modifi-
cation. The total energy at any instant is,

$$E = \text{constant} = \frac{P^2}{2\mu_{ab,cd}} + \sum_i x_i^* x_i E_i + V_{int} \qquad (31)$$

The first and second terms are the kinetic energy in the collision coordi-
nate and the internal energy respectively. The third term is the inter-
action potential which is calculated as,

$$V_{int} = \iint \Psi^*(r_1,r_2) \; V(r_1,r_2,R) \; \Psi(r_1,r_2) \partial r_1 \partial r_2$$

$$\qquad (32)$$

$$= \sum_i \sum_j x_i^* x_j \; V_{ij}$$

20

The kinetic energy in the collision coordinate, and hence the velocity are continuously modified such that Eqn. (31) remains satisfied. The relative motion is essentially governed by an effective potential which is a function of the quantum mechanical state of the internal system as well as the relative center of mass separation. The resulting path, although not optimal for any particular state-to-state probability is biased toward exit channels which play the greatest role in the inelastic scattering.

The results in column c of Table II show that modifying the classical path as described above improves the probabilities compared to case a, almost halving the errors in this case. Symmetrizing the probability matrix as before leads to the entries found in the last column of Table II. These results are in excellent agreement with the quantum mechanical probabilities. All of the semiclassical results reported below have been obtained by this procedure of imposing energy conservation and symmetrizing. Although the agreement between the quantum mechanical and semiclassical results is not always quite as striking as it is in the above example, we find that it remains very good for every case we studied. Figure III shows inelastic collision probabilities for the conditions in the sample calculation discussed above. Shown are probabilities that a system starting in a particular initial state, has a collision which is inelastic, leading collectively to any other state. That is, we are plotting one minus the retention probability. The close coupled quantum results are labeled with a "Q" and the semiclassical results are labeled with an "S". The classical results, also shown and labeled with a "C," will be discussed later. Although there are fourteen open channels at this energy, the probability of an inelastic event approaches essentially zero by about the ninth or tenth state. Figure IV corresponds to collisions at 1.0 ev, a lower total energy than Figure III.

21

Figure V corresponds to a higher energy 1.75 ev. Note that the scale of the graph has been expanded by an order of magnitude for the 1.0 ev collisions due to the small probability of inelastic scattering. For the 1.0 ev calculations, there are eight open channels. Sixteen basis states were used in the quantum calculations and fifteen in the semiclassical calculations. As seen in Figure V, there is considerably more inelastic scattering at 1.75 ev, where forty five basis states were used for both the quantum and the semiclassical calculations. Figures III-V show basically the same trends in the probabilities. Increasing the energy simply increases the amount of the inelastic scattering.

It is also instructive to compare the quantum and semiclassical results for scattering from a particular initial state. Figure VI shows such results for a collision at 1.75 ev starting in the second state, i.e., a state with the nitrogen molecule in its ground state and the oxygen molecule in its first excited state. As shown in Figure V, this is the initial state for which the semiclassical and quantum calculations show the least agreement. There is roughly equal probability for a transition to the first state and a transition to the fourth state. These correspond to transitions of the oxygen to its ground state and to its second excited state respectively. The semiclassical calculations slightly underestimate this probability in both cases. The normalization condition requires that the sum of the deviations in Figure VI vanish. It therefore follows that the retention probability is overestimated.

The more complete results of the semiclassical and quantum mechanical calculations at the three energies (1.0 ev, 1.25 ev, and 1.75 ev) are shown

22

in Tables III-V. The semiclassical state-to-state probabilities are displayed in parentheses below the quantum probabilities. The quantities plotted in Figures III, IV, and V are simply one minus the diagonal elements in these Tables. Figure VI is the second column in Table V. Not all of the twenty seven available channels are represented in Table V. One can see however that the amount of inelastic scattering is dropping off rapidly.

The classical results shown in figures III-X are all based on the quasi-classical (17) (binning) method described in section III. Transition probabilities from each specified initial state were calculated from 500 trajectories. Previous applications of the quasi-classical method have had greatest success when many final states are dynamically accessible (23). It seems reasonable to expect, therefore, that higher collision energies should begin to show better agreement between the classical results and the corresponding quantum results. By inspection of Figures III-V and also from the results at 2.25 ev shown in Figure VII, one can see that the agreement does not improve as expected. Certain state-to-state probabilities do show excellent agreement, however, and general trends in transition probabilities are modelled reasonably well. For example, for collisions at 1.75 ev. (Fig. VI), the classical estimate of the elastic scattering from the $n(O_2) = 1$, $n(N_2) = 0$ initial state is significantly less than the quantum prediction, giving rise to a classical overestimate of the inelastic scattering from that state (Fig. V). At 2.25 ev. (Fig. VIII), the elastic scattering from the ground vibrational state is in excellent agreement with the quantum results. At 2.25 ev (the highest energy considered), the classical estimate is high for inelastic scattering from initial states where nitrogen is more excited than oxygen, and it is low for initial states where oxygen is more excited than nitrogen. This trend is not apparent at lower collision energies.

23

At low collision energy (1.00 ev.), the classical binning approach shows essentially zero inelastic scattering for all initial states. This is a severe test of the binning procedure and it is normally under these low energy conditions that other classical approaches e.g., the moment method (24) or Wigner distribution methods (25) have had more success. The unbinned final actions for a set of 400 trajectories are shown in Figure VIII. It is clear that the artificial imposition of binning "boundaries" may contribute to the inadequacy of the classical results. Other procedures (such as those mentioned) may prove more useful. Work is in progress to determine the success and practicality of these other approaches.

Similar final action plots are shown in Figures IX and X for a higher collision energy (2.25 ev), where inelastic scattering dominates. The initial classical actions for the collisions represented in Fig. IX correspond to quantum state 8 and for Fig. X to quantum state 13. The energetically accessible region for this high energy system is extensive. There are 44 open channels at this energy. This means that at least 44 of the bins represented in Figures IX and X are accessible within the constraint of energy conservation. The emerging boundaries of the points in Figures IX and X show that the dynamically accessible regions are much more restricted. Figure IX for example, only 14 channels are being populuated (21 channels are populated via the corresponding quantum mechanical dynamics). Apparently, the classical dynamics precludes the possibility of populating some of these bins which correspond to states which are quantum mechanically accessible. Perhaps an alternative choice of initial condition selection (e.g., via the Wigner distribution method (25)) or analysis of final conditions (e.g., the moment method (24)) would eliminate some of the discrepencies.

VI. Summary and Discussion

As a shock passes through a condensed phase material, each molecule instantaneously feels an impulse. This impulse is the sum of the changes in the individual forces the molecule feels as each of its neighbors moves. Studying the microscopic behavior of such a system requires evaluating how a specific impulse effects a molecule, given the molecule's initial state and the impulse characteristics. To address this problem, we first need to ask about the behavior of the microscopic system, and then about a macroscopic ensemble of many such systems.

This paper addressed part of the miscroscopic question. Specifically, we asked how quantum mechanical effects influence the description of a microscopic collision, and what is a good calculation of the collision properties. We considered two harmonic oscillators interacting through a Lennard-Jones potential. This model problem is a vehicle for studying the quantum effects of discrete vibrational states on the collision of two molecules. The model problem was solved quantum mechanically by a close-coupling method, semiclassically by several variations of a classical path approach, and classically by a quasiclassical trajectory method.

The quantum mechanical calculation was considered the correct answer against which we compared the results of the classical and semiclassical calculation. The output of this calculation was the final distribution of internal states of the two molecules, once they had collided and completely separated. The quantum mechanical results were discussed in Section V.

The straightforward semiclassical classical path description discussed in Section V gave reasonable answers. However, when the path was modified to conserve energy and the microscopic reversibility was imposed on the

25

final state to state probabilities, the results were found to be in excellent agreement with the close-coupling calculations. The method faithfully reproduced the exact quantum mechanical state-to-state transition probabilities for a wide range of collision energies. This range extends from energies which produce almost no inelastic scattering to energies which produce mostly inelastic scattering. This result is encouraging since an attempt was made to choose potentials which correspond to what might be expected in a realistic molecular collision.

The classical method used in this paper is the quasi-classical trajectory method. Final values of internal coordinates (action variables) were assigned to quantum states by a simple binning procedure. The results for the final distribution of vibrational states of the molecules do not agree particularly well with the quantum and semi-classical calculations. In particular, the region of phase space required in order to populate states which are populated quantum mechanically and semiclassically appears in some cases to be dynamically inaccessable.

It is reasonable to ask whether modifying the classical approach would give better answers. For example, the quasi-classical method as implemented is not microscopically reversible. This important dynamical concept may be incorporated in the calculations by selecting the initial action variables from a uniform distribution centered around a particular quantum number. Such a microscopically reversible quasi-classical technique was used in a few of the initial states, but it showed no significant effect on the results. This is not surprising because the original batches of trajectories did not violate microscopic reversibility to any significant degree. Other approaches to final action analysis, such as the moment method, or a modified choice of initial conditions which incorporate quantum

26

effects more directly, such as the Wigner distribution method, might improve the agreement between classical and quantum results.

The encouraging result of this paper is the good agreement between the quantum and the semiclassical predictions. This introduces an interesting possibility for molecular dynamics calculations. The semiclassical calculations could be used to determine the distribution of states arising from a collision. Then this distribution could be incorporated as a submodel in a classical molecular dynamics calculation. This, however, involves several leaps of faith. First, there is a basic problem that the quantum calculation only gives the final distribution of states, in the asymptotic region of the collision. It is not at all clear how well the semiclassical calculations represent the collision in the interaction region. The premise of the molecular dynamics calculation would be that the results of an impulse felt by a molecule, due to its simultaneously interacting with many molecules, could be related to the results of an impulse of the same magnitude felt by the collision with just one molecule. Even if the answers are not equivalent, does statistical averaging make them better. These are just a few of the questions that will be addressed in the future.

Acknowledgment

27

## TABLE I

Indexing scheme for diatomic product functions. Vibrational
quantum numbers for the individual harmonic oscillator states
are shown. Note that the states are ordered in increasing energy.

| STATE INDEX | n(1) | n(2) | ENERGY (ev) |
|:---:|:---:|:---:|:---:|
| 1 | 0 | 0 | 0.2442 |
| 2 | 1 | 0 | 0.4401 |
| 3 | 0 | 1 | 0.5366 |
| 4 | 2 | 0 | 0.6360 |
| 5 | 1 | 1 | 0.7325 |
| 6 | 0 | 2 | 0.8290 |
| 7 | 3 | 0 | 0.8319 |
| 8 | 2 | 1 | 0.9284 |
| 9 | 1 | 2 | 1.0249 |
| 10 | 4 | 0 | 1.0279 |
| 11 | 0 | 3 | 1.1214 |
| 12 | 3 | 1 | 1.1244 |
| 13 | 2 | 2 | 1.2208 |
| 14 | 5 | 0 | 1.2238 |
| 15 | 1 | 3 | 1.3173 |
| 16 | 4 | 1 | 1.3203 |
| 17 | 0 | 4 | 1.4138 |
| 18 | 3 | 2 | 1.4168 |
| 19 | 6 | 0 | 1.4197 |
| 20 | 2 | 3 | 1.5133 |
| 21 | 5 | 1 | 1.5162 |
| 22 | 1 | 4 | 1.6097 |
| 23 | 4 | 2 | 1.6127 |
| 24 | 7 | 0 | 1.6156 |
| 25 | 0 | 5 | 1.7062 |
| 26 | 3 | 3 | 1.7092 |
| 27 | 6 | 1 | 1.7121 |
| 28 | 2 | 4 | 1.8057 |
| 29 | 5 | 2 | 1.8086 |
| 30 | 8 | 0 | 1.8116 |

TABLE II

Comparison of quantum mechanical state to state transition probabilities
with those calculated using a variety of semiclassical classical
path schemes for a collision with total energy 1.25 ev. starting
in the ground state.

| STATE | QUANTUM | SEMICLASSICAL | | | |
|-------|---------|------|------|------|------|
|       |         | a    | b    | c    | d    |
| 1     | .925    | .870 | .906 | .893 | .924 |
| 2     | .073    | .119 | .088 | .100 | .073 |
| 3     | .001    | .002 | .002 | .001 | .001 |
| 4     | .001    | .008 | .004 | .006 | .003 |
| 5     | .000    | .000 | .000 | .000 | .000 |
| .     | .       | .    | .    | .    | .    |
| .     | .       | .    | .    | .    | .    |
| 14    | .000    | .000 | .000 | .000 | .000 |

## TABLE III

Quantum mechanical state to state transition probabilities for model system with a total collision energy of 1.00 ev. Semiclassical; probabilities (see text) are shown in parentheses. There are eight open (energetically accessible) channels at this energy.

|   | 1 | 2 | 3 | 4 | 5 | 6 | 7 | 8 |
|---|---|---|---|---|---|---|---|---|
| 1 | .981 | .019 | .000 | .000 | .000 | .000 | .000 | .000 |
|   | (.978) | (.022) | (.000) | (.000) | (.000) | (.000) | (.000) | (.000) |
| 2 | .019 | .967 | .008 | .006 | .000 | .000 | .000 | .000 |
|   | (.022) | (.962) | (.006) | (.010) | (.000) | (.000) | (.000) | (.000) |
| 3 | .000 | .008 | .991 | .000 | .001 | .000 | .000 | .000 |
|   | (.000) | (.006) | (.992) | (.000) | (.002) | (.000) | (.000) | (.000) |
| 4 | .000 | .006 | .000 | .990 | .004 | .000 | .000 | .000 |
|   | (.000) | (.010) | (.000) | (.986) | (.003) | (.000) | (.001) | (.000) |
| 5 | .000 | .000 | .001 | .004 | .994 | .001 | .000 | .000 |
|   | (.000) | (.000) | (.002) | (.003) | (.994) | (.001) | (.000) | (.000) |
| 6 | .000 | .000 | .000 | .000 | .001 | .999 | .000 | .000 |
|   | (.000) | (.000) | (.000) | (.000) | (.001) | (.999) | (.000) | (.000) |
| 7 | .000 | .000 | .000 | .000 | .000 | .000 | 1.00 | .000 |
|   | (.000) | (.000) | (.000) | (.001) | (.000) | (.000) | (.999) | (.000) |
| 8 | .000 | .000 | .000 | .000 | .000 | .000 | .000 | 1.00 |
|   | (.000) | (.000) | (.000) | (.000) | (.000) | (.000) | (.000) | (1.00) |

## TABLE IV

Same as TABLE III with a total collision energy of 1.25 ev. There are fourteen open channels.

| | 1 | 2 | 3 | 4 | 5 | 6 | 7 | 8 | 9 | 10 | 11 | 12 | 13 | 14 |
|---|---|---|---|---|---|---|---|---|---|---|---|---|---|---|
| 1 | .925 | .073 | .001 | .001 | .000 | .000 | .000 | .000 | .000 | .000 | .000 | .000 | .000 | .000 |
| | (.924) | (.073) | (.001) | (.003) | (.000) | (.000) | (.000) | (.000) | (.000) | (.000) | (.000) | (.000) | (.000) | (.000) |
| 2 | .073 | .854 | .020 | .051 | .001 | .000 | .000 | .000 | .000 | .000 | .000 | .000 | .000 | .000 |
| | (.073) | (.855) | (.014) | (.055) | (.001) | (.000) | (.002) | (.000) | (.000) | (.000) | (.000) | (.000) | (.000) | (.000) |
| 3 | .001 | .020 | .964 | .001 | .014 | .000 | .000 | .000 | .000 | .000 | .000 | .000 | .000 | .000 |
| | (.001) | (.014) | (.967) | (.001) | (.017) | (.000) | (.000) | (.000) | (.000) | (.000) | (.000) | (.000) | (.000) | (.000) |
| 4 | .001 | .051 | .001 | .910 | .020 | .000 | .016 | .000 | .000 | .000 | .000 | .000 | .000 | .000 |
| | (.003) | (.055) | (.001) | (.903) | (.015) | (.000) | (.022) | (.000) | (.000) | (.000) | (.000) | (.000) | (.000) | (.000) |
| 5 | .000 | .001 | .014 | .020 | .951 | .010 | .000 | .004 | .000 | .000 | .000 | .000 | .000 | .000 |
| | (.000) | (.001) | (.017) | (.015) | (.952) | (.008) | (.000) | (.006) | (.000) | (.000) | (.000) | (.000) | (.000) | (.000) |
| 6 | .000 | .000 | .000 | .000 | .010 | .989 | .000 | .000 | .000 | .000 | .000 | .000 | .000 | .000 |
| | (.000) | (.000) | (.000) | (.000) | (.008) | (.991) | (.000) | (.000) | (.001) | (.000) | (.000) | (.000) | (.000) | (.000) |
| 7 | .000 | .000 | .000 | .016 | .000 | .000 | .972 | .009 | .000 | .001 | .000 | .000 | .000 | .000 |
| | (.000) | (.002) | (.000) | (.022) | (.000) | (.000) | (.965) | (.008) | (.000) | (.004) | (.000) | (.000) | (.000) | (.000) |
| 8 | .000 | .000 | .000 | .000 | .004 | .000 | .009 | .983 | .004 | .000 | .000 | .000 | .000 | .000 |
| | (.000) | (.000) | (.000) | (.000) | (.006) | (.000) | (.008) | (.981) | (.004) | (.000) | (.000) | (.001) | (.000) | (.000) |
| 9 | .000 | .000 | .000 | .000 | .000 | .000 | .000 | .004 | .995 | .000 | .001 | .000 | .000 | .000 |
| | (.000) | (.000) | (.000) | (.000) | (.000) | (.001) | (.000) | (.004) | (.995) | (.000) | (.001) | (.000) | (.000) | (.000) |
| 10 | .000 | .000 | .000 | .000 | .000 | .000 | .001 | .000 | .000 | .998 | .000 | .001 | .000 | .000 |
| | (.000) | (.000) | (.000) | (.000) | (.000) | (.000) | (.004) | (.000) | (.000) | (.995) | (.000) | (.001) | (.000) | (.000) |
| 11 | .000 | .000 | .000 | .000 | .000 | .000 | .000 | .000 | .001 | .000 | .999 | .000 | .000 | .000 |
| | (.000) | (.000) | (.000) | (.000) | (.000) | (.000) | (.000) | (.000) | (.001) | (.000) | (.999) | (.000) | (.000) | (.000) |
| 12 | .000 | .073 | .000 | .000 | .000 | .000 | .000 | .000 | .000 | .001 | .000 | .999 | .000 | .000 |
| | (.000) | (.000) | (.000) | (.000) | (.000) | (.000) | (.000) | (.001) | (.000) | (.001) | (.000) | (.998) | (.000) | (.000) |
| 13 | .000 | .000 | .000 | .000 | .000 | .000 | .000 | .000 | .000 | .000 | .000 | .000 | 1.00 | .000 |
| | (.000) | (.000) | (.000) | (.000) | (.000) | (.000) | (.000) | (.000) | (.000) | (.000) | (.000) | (.000) | (1.00) | (.000) |
| 14 | .000 | .000 | .000 | .000 | .000 | .000 | .000 | .000 | .000 | .000 | .000 | .000 | .000 | 1.00 |
| | (.000) | (.000) | (.000) | (.000) | (.000) | (.000) | (.000) | (.000) | (.000) | (.000) | (.000) | (.000) | (.000) | (1.00) |

## TABLE V

Same as TABLE III with a total collision energy of 1.75 ev. Although there are 27 open channels at this energy, only results for the first 14 are shown here. One can see from FIG. V that the probability of an inelastic collision decreases considerably for higher states.

| | 1 | 2 | 3 | 4 | 5 | 6 | 7 | 8 | 9 | 10 | 11 | 12 | 13 | 14 |
|---|---|---|---|---|---|---|---|---|---|---|---|---|---|---|
| 1 | .677 (.708) | .282 (.246) | .005 (.003) | .034 (.036) | .001 (.001) | .000 (.000) | .001 (.005) | .000 (.000) | .000 (.000) | .000 (.001) | .000 (.000) | .000 (.000) | .000 (.000) | .000 (.000) |
| 2 | .282 (.246) | .354 (.417) | .035 (.021) | .280 (.259) | .016 (.011) | .000 (.000) | .030 (.039) | .001 (.003) | .000 (.000) | .001 (.005) | .000 (.000) | .000 (.000) | .000 (.000) | .000 (.000) |
| 3 | .005 (.003) | .035 (.021) | .786 (.811) | .016 (.009) | .148 (.140) | .002 (.002) | .001 (.001) | .007 (.011) | .000 (.000) | .000 (.000) | .000 (.000) | .000 (.001) | .000 (.000) | .000 (.000) |
| 4 | .034 (.036) | .280 (.259) | .016 (.009) | .363 (.491) | .044 (.029) | .001 (.000) | .231 (.222) | .016 (.012) | .000 (.000) | .014 (.026) | .000 (.000) | .001 (.002) | .000 (.000) | .000 (.002) |
| 5 | .001 (.001) | .016 (.011) | .148 (.140) | .044 (.029) | .593 (.634) | .043 (.028) | .017 (.011) | .128 (.130) | .006 (.006) | .001 (.001) | .000 (.000) | .003 (.008) | .000 (.000) | .000 (.000) |
| 6 | .000 (.000) | .000 (.000) | .002 (.002) | .001 (.000) | .043 (.028) | .897 (.910) | .000 (.000) | .006 (.004) | .051 (.053) | .000 (.000) | .000 (.001) | .000 (.000) | .000 (.0002) | .000 (.000) |
| 7 | .001 (.005) | .030 (.039) | .001 (.001) | .231 (.222) | .017 (.011) | .000 (.000) | .503 (.513) | .053 (.037) | .001 (.001) | .151 (.152) | .000 (.000) | .008 (.009) | .000 (.000) | .003 (.011) |
| 8 | .000 (.000) | .001 (.003) | .007 (.011) | .016 (.012) | .128 (.130) | .006 (.004) | .053 (.037) | .648 (.671) | .053 (.039) | .010 (.006) | .000 (.000) | .074 (.080) | .003 (.004) | .000 (.000) |
| 9 | .000 (.000) | .000 (.000) | .000 (.000) | .000 (.000) | .006 (.006) | .051 (.053) | .001 (.001) | .053 (.039) | .828 (.843) | .000 (.000) | .027 (.020) | .004 (.003) | .029 (.034) | .000 (.000) |
| 10 | .000 (.001) | .001 (.005) | .000 (.000) | .014 (.026) | .001 (.001) | .000 (.000) | .151 (.152) | .010 (.006) | .000 (.001) | .707 (.695) | .000 (.000) | .049 (.036) | .001 (.000) | .064 (.072) |
| 11 | .000 (.000) | .000 (.000) | .000 (.000) | .000 (.000) | .000 (.000) | .000 (.001) | .000 (.000) | .000 (.000) | .027 (.020) | .000 (.000) | .964 (.969) | .000 (.000) | .001 (.000) | .000 (.000) |
| 12 | .000 (.000) | .000 (.000) | .000 (.001) | .001 (.002) | .003 (.008) | .000 (.000) | .008 (.009) | .074 (.080) | .004 (.003) | .049 (.036) | .000 (.000) | .787 (.791) | .045 (.034) | .003 (.002) |
| 13 | .000 (.000) | .000 (.000) | .000 (.000) | .000 (.000) | .000 (.001) | .000 (.002) | .000 (.000) | .003 (.004) | .029 (.034) | .001 (.000) | .001 (.000) | .045 (.035) | .888 (.893) | .000 (.000) |
| 14 | .000 (.000) | .000 (.000) | .000 (.000) | .000 (.002) | .000 (.000) | .000 (.000) | .003 (.011) | .000 (.000) | .000 (.000) | .064 (.072) | .000 (.000) | .003 (.002) | .000 (.000) | .387 (.872) |
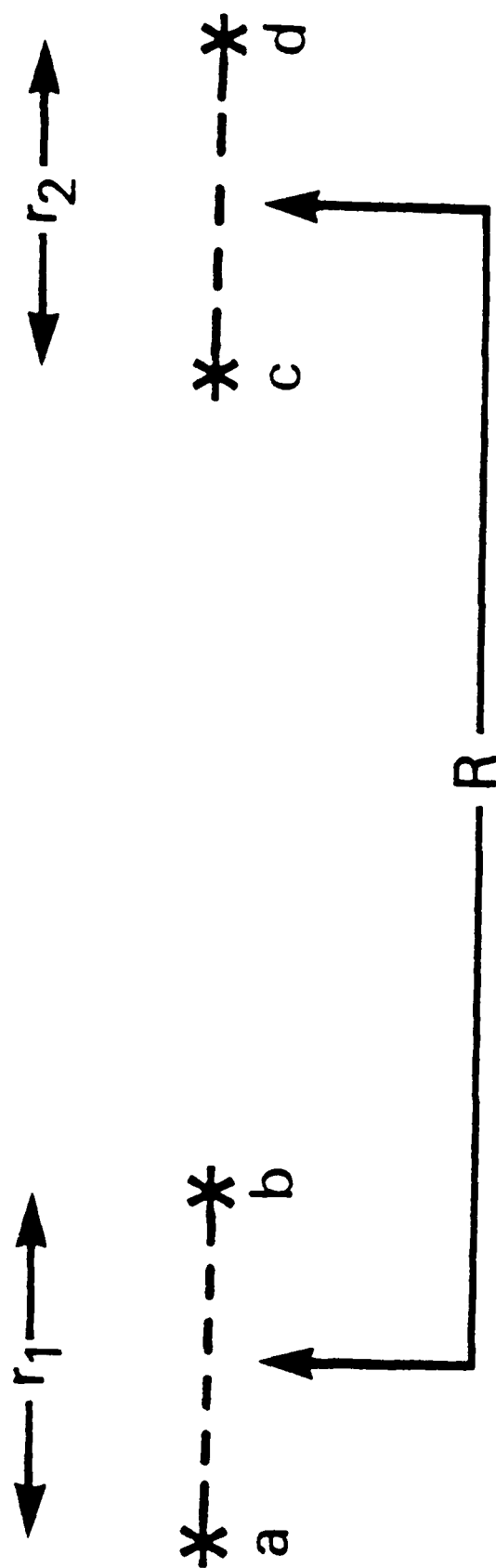
FIG. I

The model diatom-diatom system. Masses and force constants for molecule a-b are chosen to correspond to those of the oxygen molecule, c-d to the nitrogen molecule.
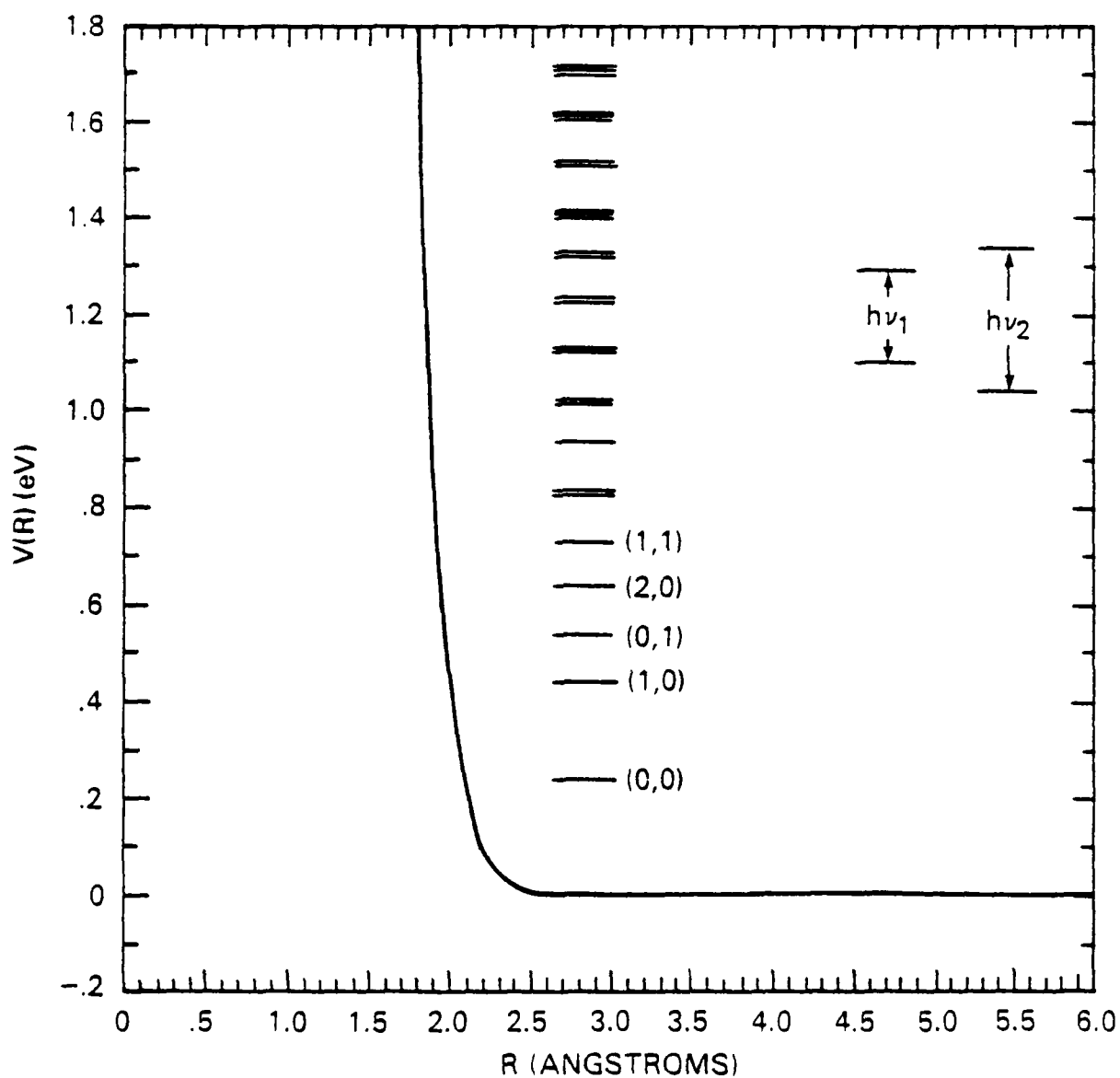
FIG. II

Intermolecular Lennard-Jones potential for model diatom-diatom system.
energy spacings for the collision partners and the first several energy
levels for the combined system are shown on the same energy scale
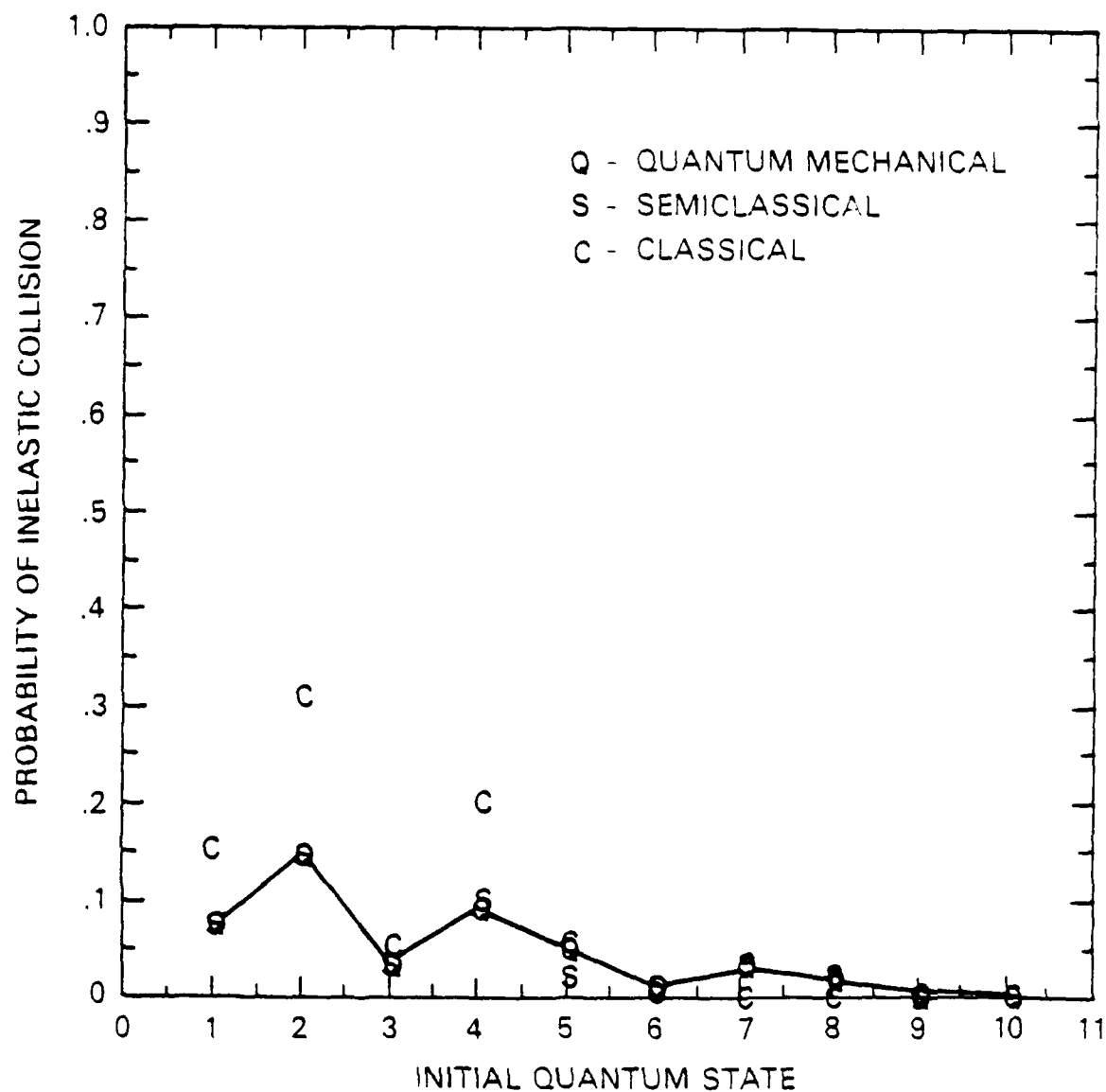for comparison.

FIG. III

Total probability of an inelastic event for a collision energy of 1.25 ev.
Shown are probabilities predicted by quantum mechanical close coupling
calculations (Q), semiclassical classical path calculations (S) and
classical trajectory calculations using the histogram binning technique (C).
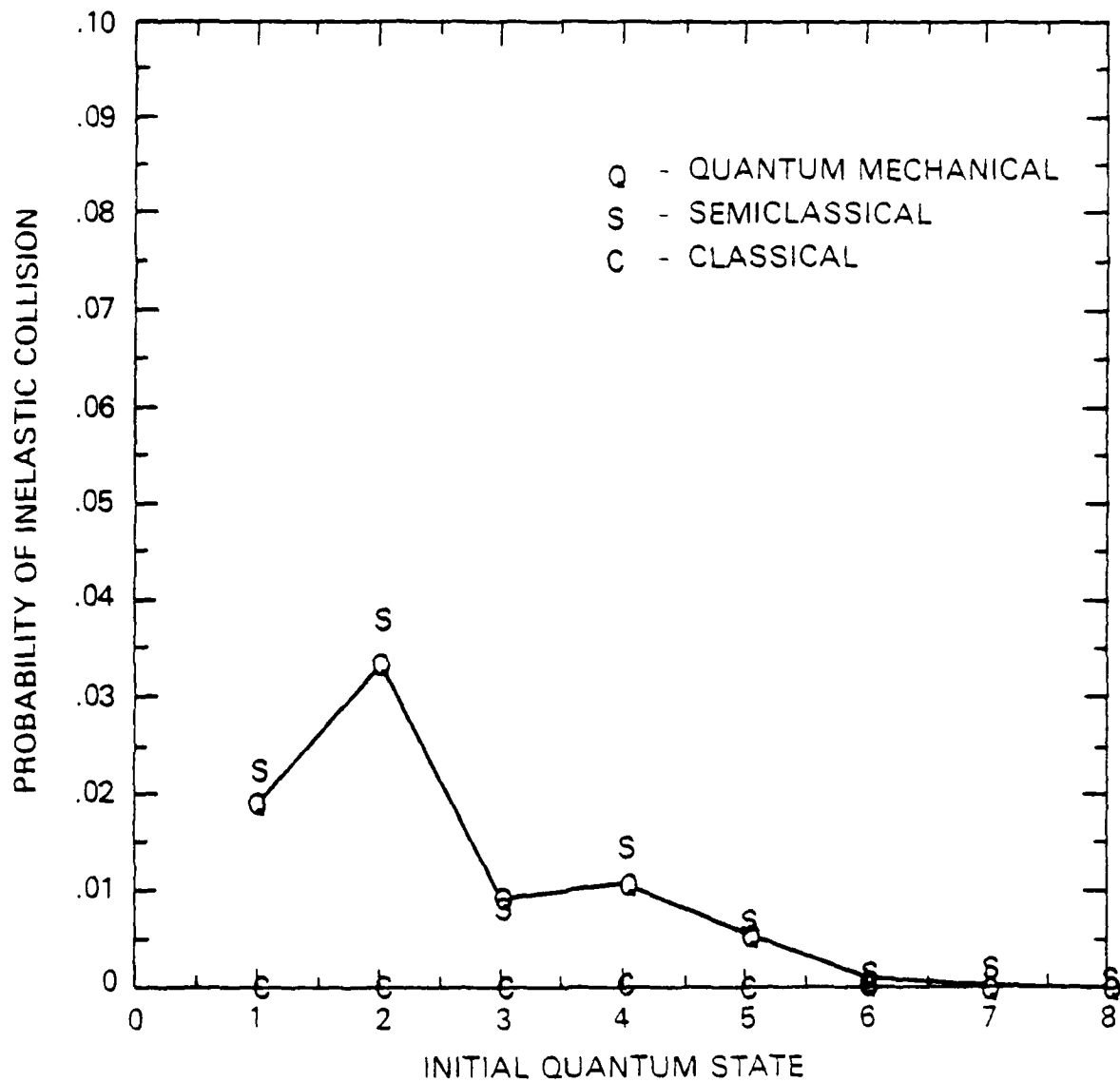
FIG. IV

Same as FIG. III, except with a lower collision energy of 1.00 ev.
Note the expanded scale.
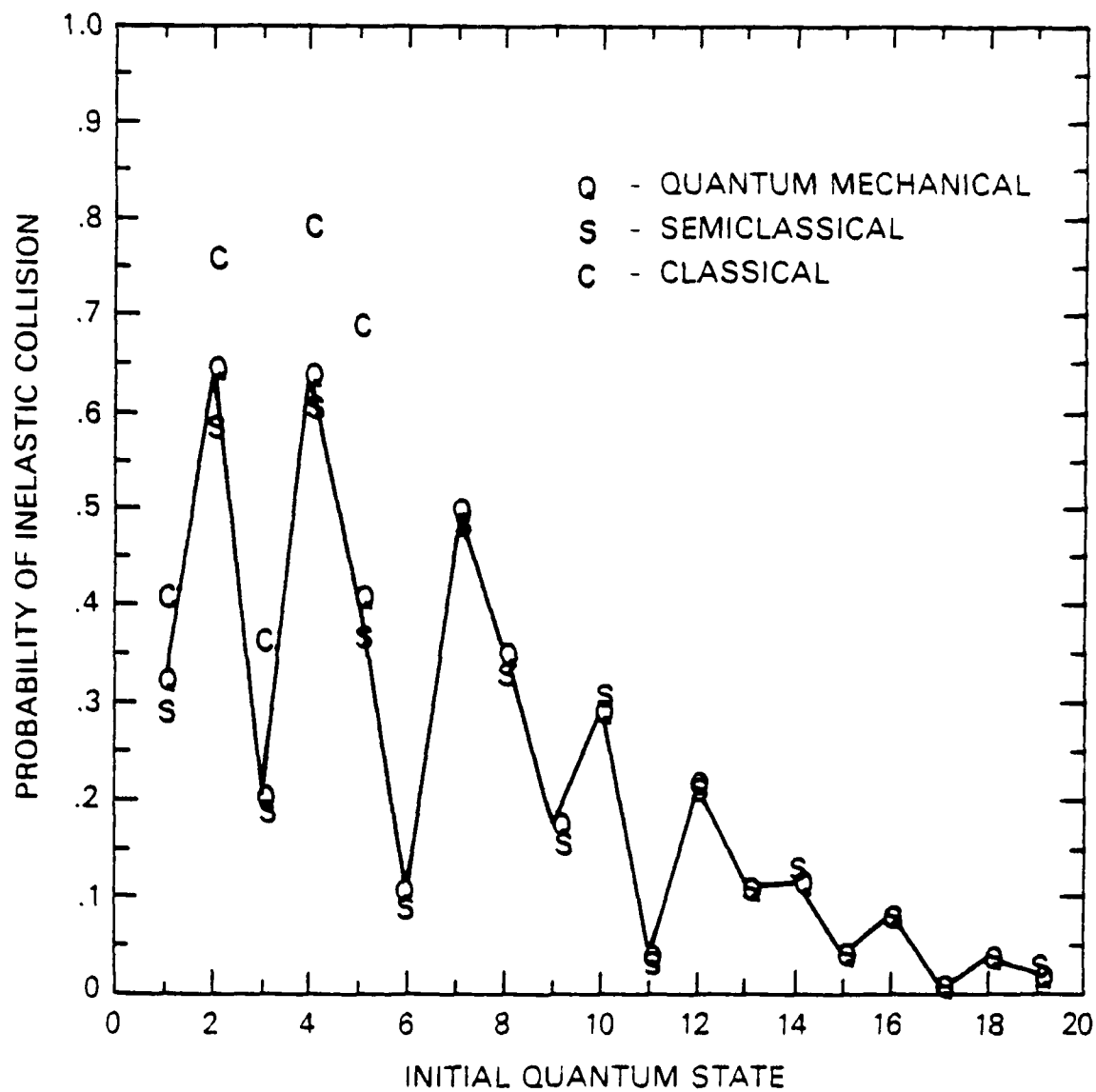
FIG. V

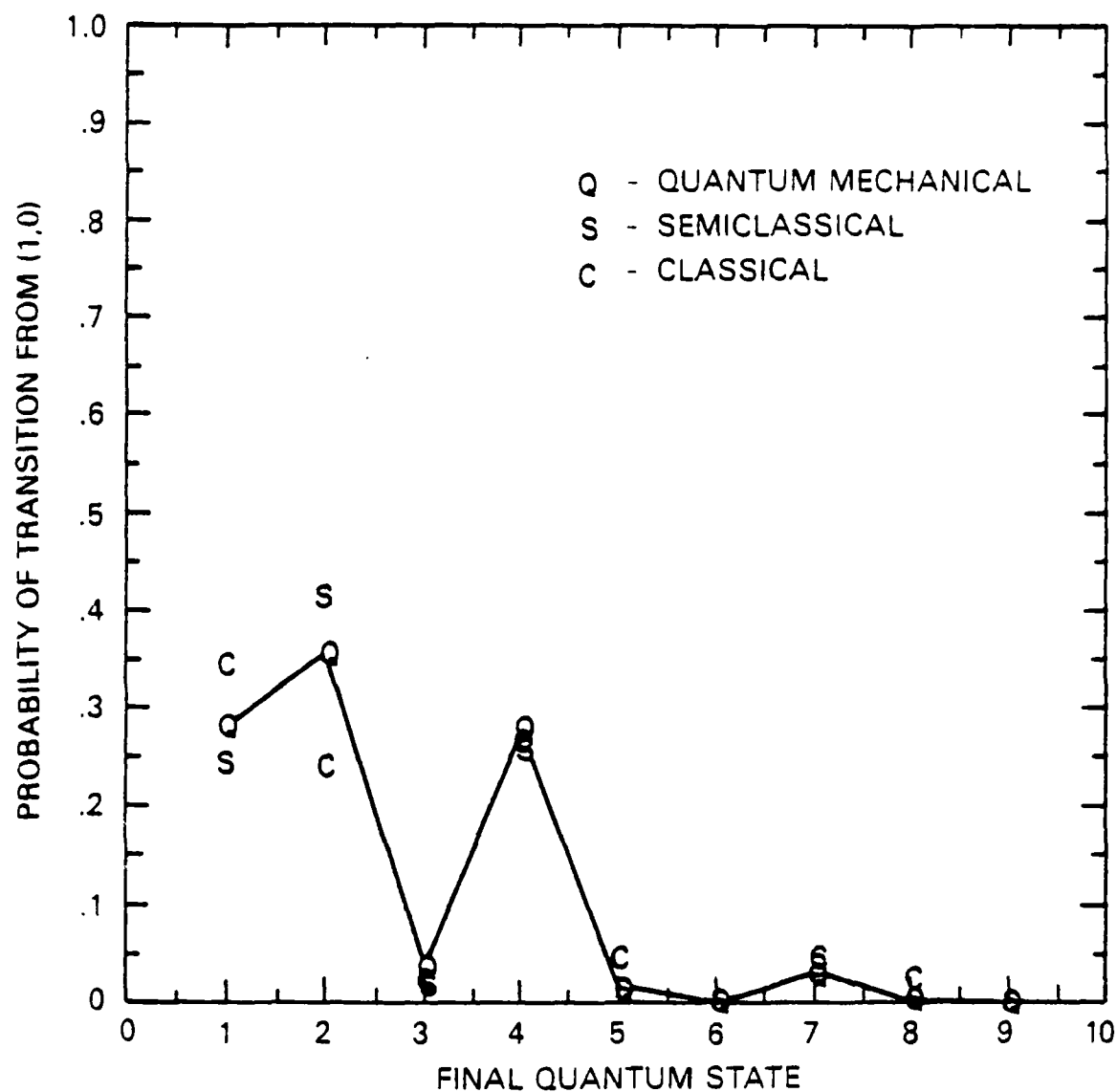Same as FIG. III except with a higher collision energy of 1.75 ev.

FIG. VI

State-to-state transition probabilities for a 1.75 ev collision
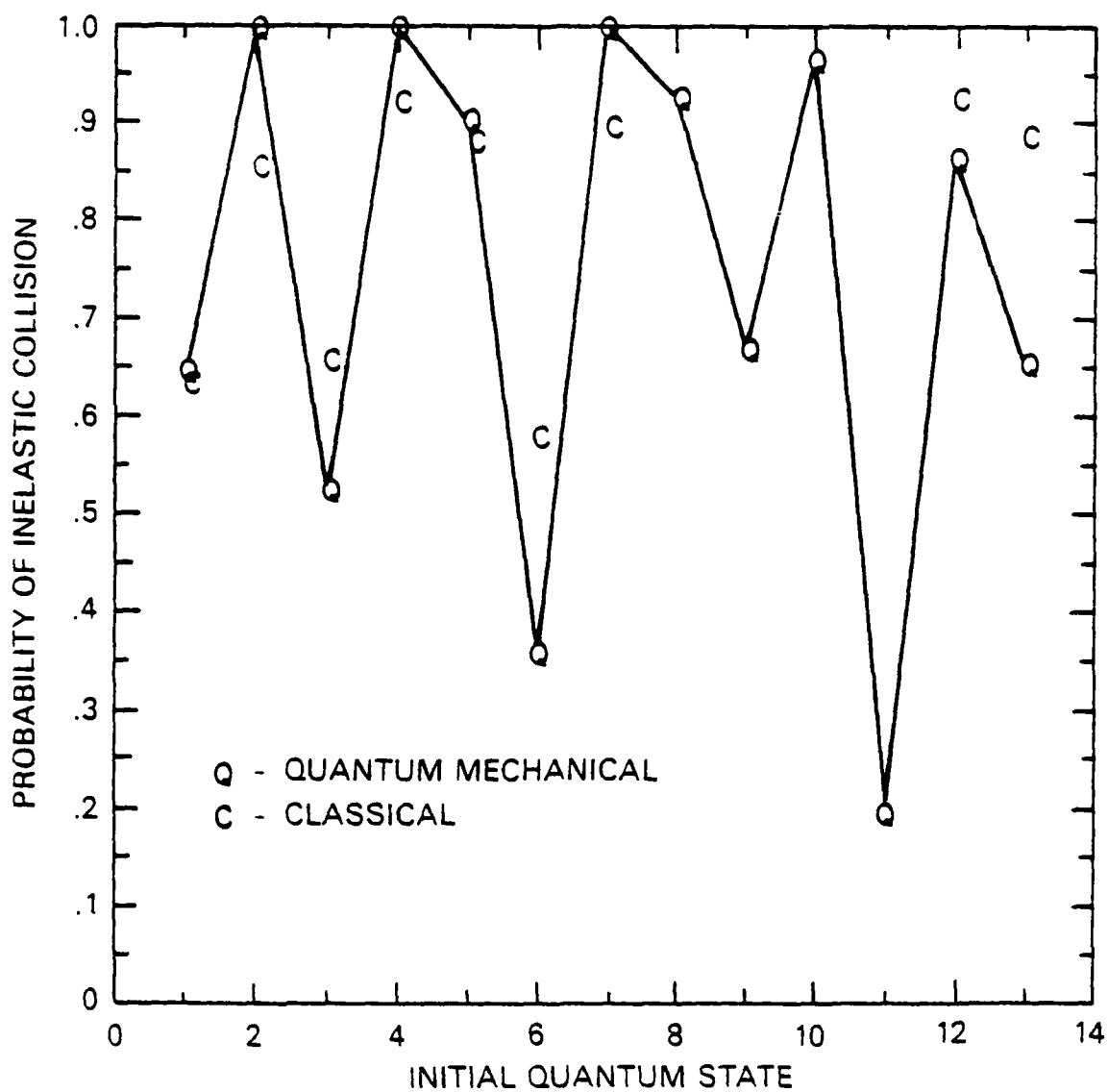beginning in the second entrance channel.

38

FIG. VII

Classical vs. quantum mechanical probabilities of inelastic
collision for a total collision energy of 2.25 ev. Note that the
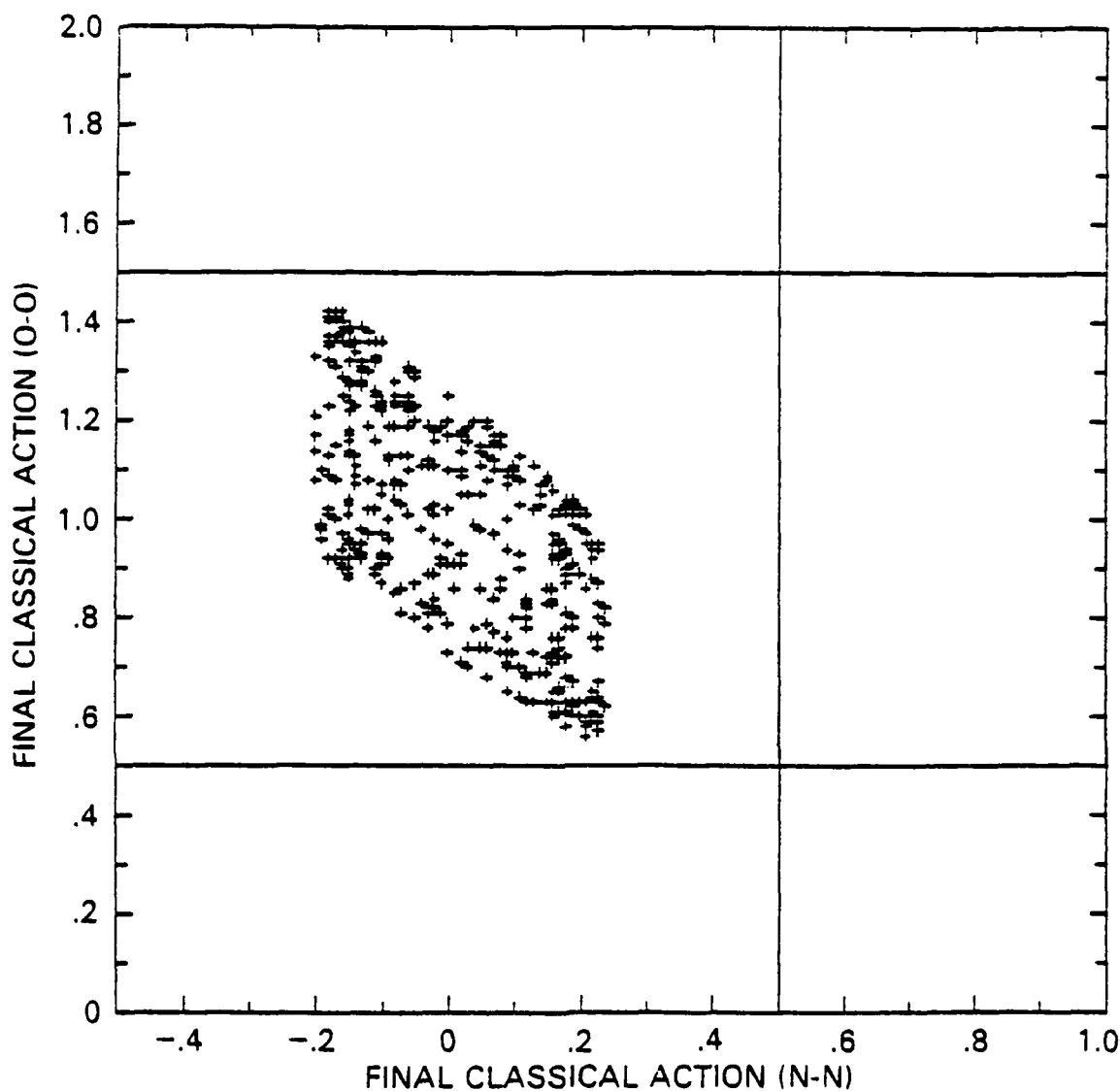scattering is predominantly inelastic at this high energy.

39

FIG. VIII

Distribution of final values of classical action variables for
collisions at 1.0 ev. The initial values of the action variables
for all trajectories are oxygen: 1.0, nitrogen: 0.0 corresponding
to quantum state 2. The initial phases of the oscillators are
chosen randomly between 0. and 2 . The grid represents the
assignment to quantum states. The quasi-classical binning technique
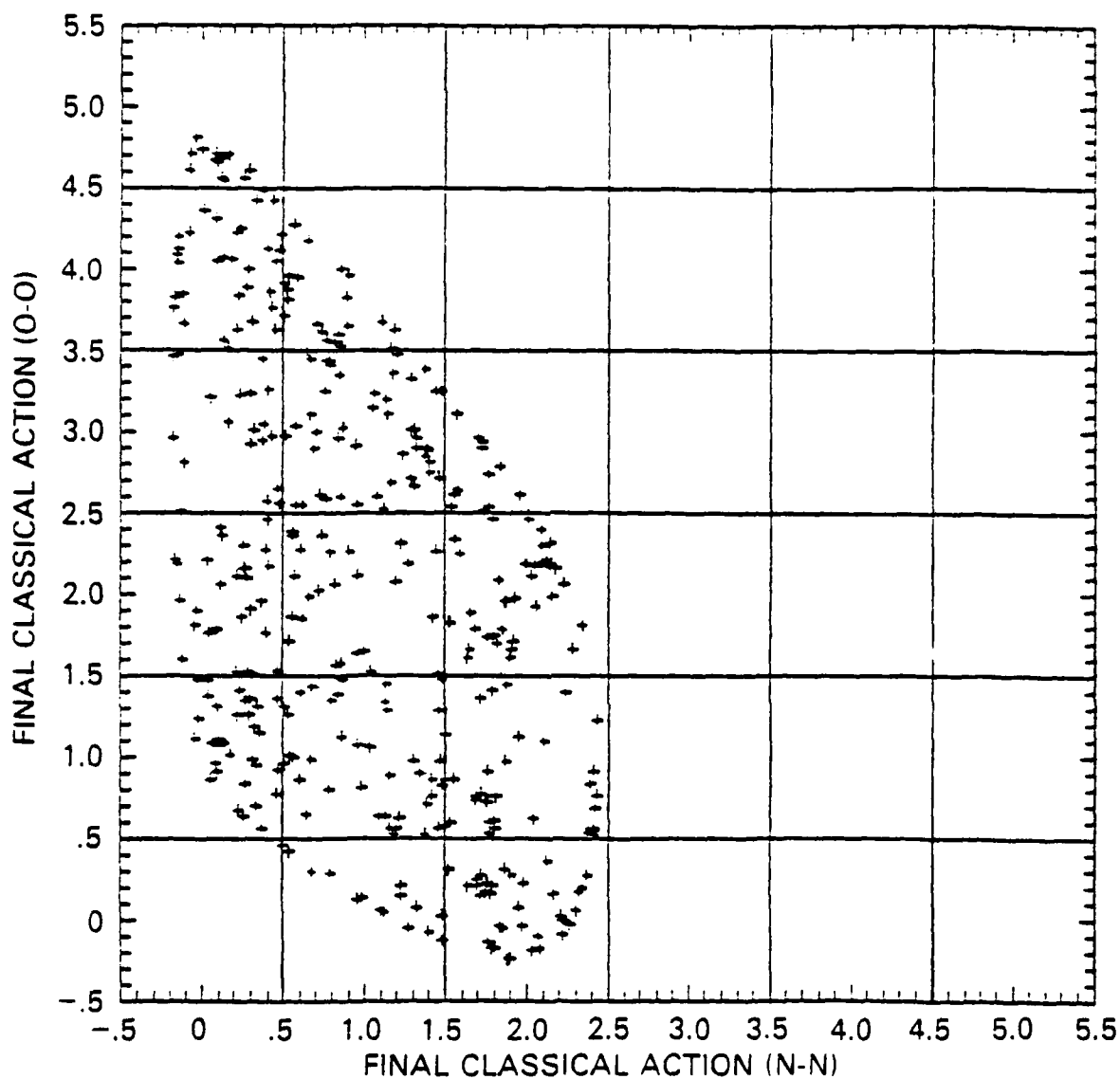predicts only elastic scattering in this case.

40

FIG. IX

Distribution of final values of classical action variables at 2.25 ev..
The initial values of the action variables for all trajectories
are oxygen: 2.0, nitrogen: 1.0 corresponding to quantum state 8.
The initial phases of the oscillators are chosen randomly between
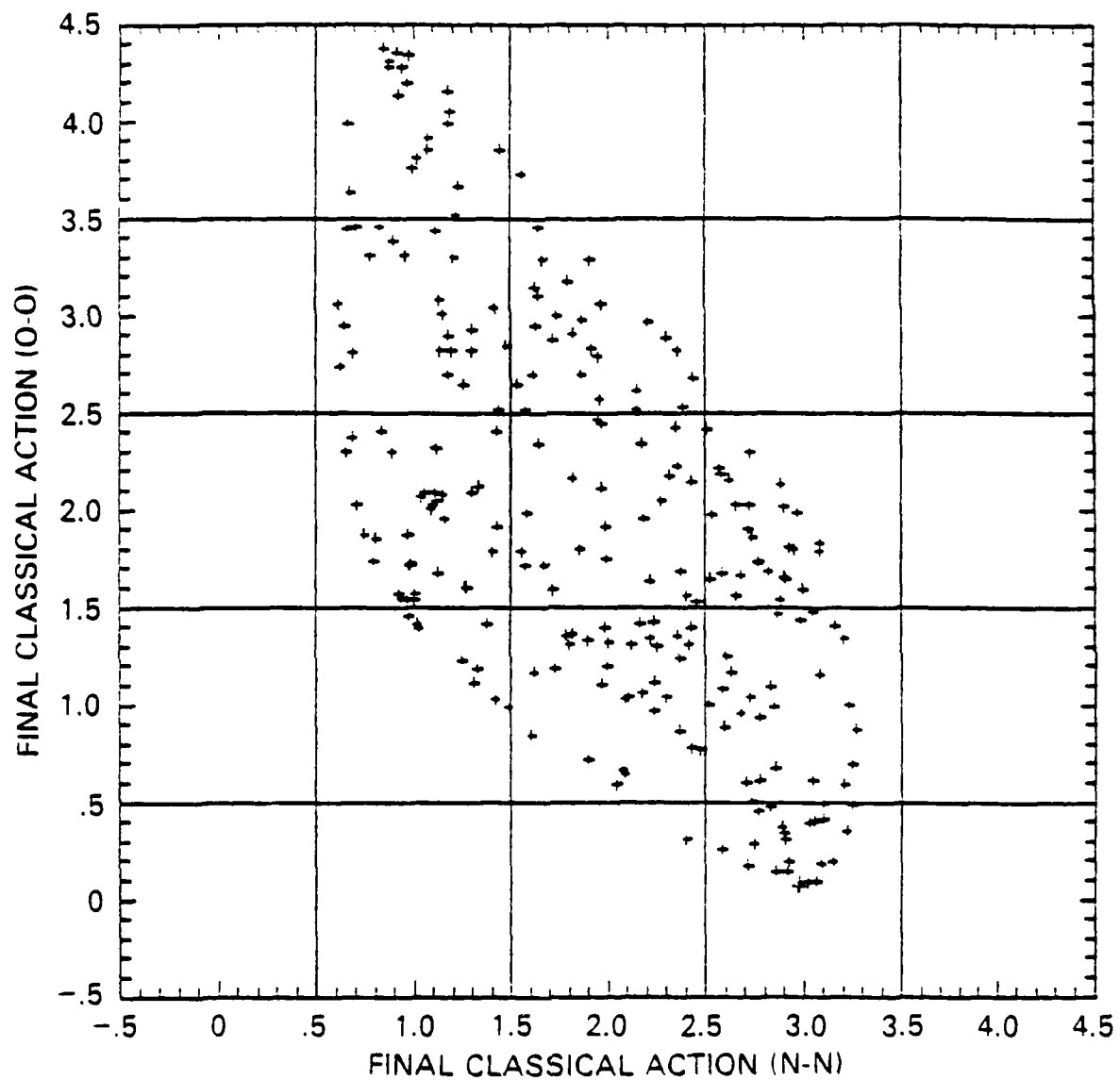0. and 2 . The grid represents the assignment to quantum states.

41

FIG. X

Same as Figure IX except that the initial classical action variables correspond to quantum state 13.

References:

1.  (a).  B.J. Alder, T.E. Wainwright, in "Transport Processes in
            Statistical Mechanics", Symp. Proc. Brussels, 1956, ed. I.
            Prigogine, p. 97, New York: Interscience
    (b).  W.J. Hoover, A.J.C. Ladd, R.B. Hickman, B.L. Holian, Phys. Rev. A
            21, 1756 (1980)
    (c).  W.G. Hoover, D.J. Evans, R.B. Hickman, A.J.C. Ladd, W.T. Ashurst,
            B. Moran, Phys. Rev. A 22, 1690 (1980)
    (d).  G. Ciccotti, G. Jacucci, Phys. Rev. Lett 35, 789 (1975)
    (e).  B.R. Sundheim, Chem. Phys. Lett 60, 427 (1979)
    (f).  E.L. Pollock, B.J. Alder, Physica A 102, 1 (1980)
    (g).  R.O.W. Watts, Chem. Phys. Lett. 80, 211 (1981)

2.  (a).  V. Yu. Klimenko, A.N. Dremin, Sov. Phys. Dokl. 24, 984 (1979)
    (b).  V. Yu. Klimenko, A.N. Dremin, Sov. Phys. Dokl. 25, 289 (1980)
    (c).  B.L. Holian, W.G. Hoover, B. Moran, G.K. Straub, Phys. Rev. A
            22, 2798 (1980)
    (d).  B.L. Holian, G.K. Straub, Phys. Rev. Lett. 43, 1598 (1979)

3.  For reviews and leading references see:  W.G. Hoover, Ann. Rev. Phys.
    Chem. 34, 103 (1983), W.W. Wood, J.J. Erpenbeck, ibid. 27, 319 (1976),
    A.N. Lagar'kov, V.M. Sergeev, Sov. Phys. Dokl. 21, 566 (1978), W.G.
    Hoover, W.T. Ashurst, Adv. Theor. Chem. 1, 1 (1975)

4.  W.H. Miller, J. Chem. Phys, 54, 5386 (1971)

5.  J.P. Ryckaert, G. Ciccotti, H.J.C. Berendsen, J. Comp. Phys. 23, 327
    (1977)

6.  Some examples are:
    (a).  P.S.Y. Cheung, J.G. Powles, Molec. Phys. 32, 1383 (1976),
    (b).  C.S. Murphy, K. Singer, I.R. McDonald, Molec. Phys. 44, 135
            (1981),
    (c).  T.H. Dorfmuller, J. Samios, Molec. Phys. 53, 1167 (1984),
    (d).  S. Murrad, K.E. Gubbins, D.J. Tildesley, Molec. Phys. 37, 725
            (1979),
    (e).  H.J. Bohm, P.A. Madden, R.M. Lyndon-Bell, I.R. McDonald, Molec.
            Phys. 51, 761 (1984);
    (f).  H.J. Bohm, C. Meissner, R. Ahlrichs, Molec. Phys. 53, 651 (1984)

7.  A. Rahman, F.H. Stillinger, J. Chem. Phys. 55, 3336 (1971)

8.  G.D. Barg, G.M. Kendall, J.P. Toennies, Chem. Phys. 16, 243 (1976), P.
    Pechukas, M.S. Child, Mol. Phys. 31, 973 (1976)

9.  J.D. Johnson, M.S. Shaw, B.L. Holian, J. Chem. Phys. 80, 3 (1984)
10. D.H. Tsai, S.F. Trevino, J. Chem. Phys. 79, 1684 (1983), S.F. Trevino,
    D.H. Tsai, ibid. 81, 1 (1984)
11. M. Bishop, M.H. Kalos, H.L. Frisch, J. Chem. Phys. 70, 1299 (1979)

12. W.H. Miller, Adv. Chem. Phys. 25, 69 (1974); W.H. Miller, Adv. Chem. Phys. 30, 77 (1976)

13. E.A. McCullough, Jr., R.E. Wyatt, J. Chem. Phys. 54, 3578 (1972); A. Kupperman, J.T. Adams, D.G. Truhlar, ICPEAC Abstracts VIII, 141, (1973); R.E. Wyatt in "State to State Chemistry", edited by P.R. Brooks and E.F. Hayes, ACS Symp. Series, 56, 185 (1977)

14. A. Lane, R. Thomas, Rev. Mod. Phys. 30, 257 (1958); J. Light, R.B. Walker, J. Chem. Phys, 65, 4272 (1976)

15. M.S. Child, "Molecular Collision Theory" (Academic Press, New York, 1974)

16. R.N. Porter and L.M. Raff in "Modern Theoretical Chemistry", edited by W.H. Miller, p. 1, (Plenum, New York, 1976)

17. M.D. Pattengill in "Atomic-Molecular Collision Theory", edited by R.B. Bernstein, p. 359, (Plenum, New York, 1979)

18. M. Born, "The Mechanics of the Atom" (Ungar, New York, 1960)

19. F.H. Mies, J. Chem. Phys. 40, 523 (1964); F.H. Mies, J. Chem. Phys. 41, 903 (1964)

20. T.L. Cottrell, J.C. McCoubrey, "Molecular Energy Transfer in Gases" (Butterworth, London, 1961)

21. R.L. McKenzie, J. Chem. Phys. 63, 1655 (1975)

22. K.J. McCann, M.R. Flannery, J. Chem. Phys. 69, 5275 (1978)

23. A.E. Orel, D.P. Ali, W.H. Miller, Chem. Phys. Lett. 79, 137 (1981)

24. See ref. (23), also:
    (a). D.G. Truhlar, N.C. Blais, J. Chem. Phys. 67, 1532 (1977);
    (b). N.C. Blais, D.G. Truhlar, J. Chem. Phys, 67, 1540 (1977);
    (c). D.G. Truhlar, J.W. Duff, Chem. Phys. Lett. 36, 551 (1975);
    (d). D.G. Truhlar, B.P. Reid, D.E. Zuraski, J.C. Gray, J. Phys. Chem., 85, 786, (1981)

25. H.W. Lee, M.O. Scully, J. Chem. Phys. 73, 2238 (1980)
26. H. Goldstein, "Classical Mechanics" (Addison Wesley, 1950)

# END

# FILMED

1-86

# DTIC